Published in final edited form as:
Pharm Res. 2013 May ; 30(5): 1447–1457. doi:10.1007/s11095-013-0986-7.

Synthetic FXR Agonist GW4064 Prevents Diet-induced Hepatic Steatosis and Insulin Resistance

Yongjie Ma[a], **Yixuan Huang**[b], **Linna Yan**[a], **Mingming Gao**[a], and **Dexi Liu**[a,*]

[a]Department of Pharmaceutical and Biomedical Sciences, College of Pharmacy, University of Georgia, Athens, Georgia 30602

[b] Department of Pharmaceutical Sciences, School of Pharmacy, University of Pittsburgh, Pittsburgh, Pennsylvania 15261

Abstract

The nuclear receptor farnesoid X receptor (FXR), an endogenous sensor for bile acids, plays an important role in cholesterol, lipid and carbohydrate metabolism. The objective of this study is to examine the effect of FXR activation on diet-induced obesity and hepatic steatosis. Activation of FXR by its synthetic agonist, 3-[2-[2-Chloro-4-[[3-(2,6-dichlorophenyl)-5-(1-methylethyl)-4-isoxazolyl]methoxy]phenyl]ethenyl]benzoic acid (GW4064), suppressed weight gain in C57BL/6 mice fed with either a high-fat diet (HFD) or high-fat, high-cholesterol diet. GW4064 treatment of mice on HFD significantly repressed diet-induced hepatic steatosis as evidenced by lower triglyceride and free fatty acid level in the liver. Analysis of genes involved in lipid metabolism showed GW4064 markedly reduced lipid transporter CD36 expression without affecting expression of genes that are directly involved in lipogenesis. GW4064 treatment attenuated hepatic inflammation while having no effect on white adipose tissue. In addition, activation of FXR by GW4064 avoided diet-induced hyperinsulinemia and hyperglycemia through decreasing the transcript levels of phosphoenolpyruvate carboxykinase *(Pepck*) and glucose-6-phosphatase (*G6pase*), two key enzymes in gluconeogenesis. These results verify the important function of FXR in diet-induced obesity and suggest that FXR agonists are promising therapeutic agents for obesity-associated metabolic disorders.

Keywords

Obesity; farnesoid X receptor; hepatic steatosis; glucose homeostasis

Introduction

Farnesoid X receptor (FXR, also known as bile acid receptor or BAR) is a ligand-activated receptor belonging to the nuclear receptor superfamily. It is highly expressed in the liver, intestine, kidney and adrenal gland and is expressed in the heart and adipose tissue as well (1). Bile acids are believed to be the endogenous ligands for FXR (2, 3). FXR has a critical role in maintaining bile acid and cholesterol homeostasis through controlling hepatic cholesterol catabolism, bile acid synthesis and intestinal absorption (4-6).

*Correspondence should be addressed: Dexi Liu, PhD, Department of Pharmaceutical and Biomedical Science, University of Georgia College of Pharmacy, Room 450 Pharmacy South, 250 West Green Street, Athens, GA 30602. Telephone: +01 706-542-7385; Fax: +01 706-542-5358; dliu@uga.edu.

Disclosures
The authors have no conflict of interest, financial or otherwise, to disclose.

In recent years, the role of FXR in lipid and glucose metabolism has been explored. FXR activation lowered plasma and liver triglyceride by enhancing plasma triglyceride clearance (7, 8) and repressing sterol regulatory element–binding protein (SREBP) 1c-mediated hepatic lipogenesis (9). Elevated serum glucose and impaired insulin tolerance have been detected in FXR-null mice fed with normal diet (10). In Zucker (*fa/fa*) obese rats, *ob/ob* mice and diabetic *db/db* mice, activation of FXR improved lipid metabolism and insulin sensitivity (11-13), suggesting that activation of FXR by agonist could be an attractive pharmacological strategy for managing diet-induced obesity and obesity-associated complications. By contrast, more recent studies using FXR knockout mice show that FXR deficiency protected mice from high-fat diet-induced obesity and improved glucose homeostasis (14, 15).

In this study, we examined the potent effects of chronic activation of FXR by its agonist GW4064 on protection of mice from development of high-fat die-induced obesity and insulin resistance. We also investigated the possible role of GW4064 in blocking diet induced hepatic steatosis. Finally, we tested the direct effects of GW4064 on expression of genes responsible for maintaining metabolic homeostasis. Our data demonstrate that FXR activation suppresses diet-induced hepatic steatosis and insulin resistance by suppressing expression of fatty acid transporter CD36 gene.

Materials and Methods

Materials

GW4064 was synthesized according to a previous report (16). Oleic acid was purchased from Sigma-Aldrich (St. Louis, MO). Fatty acid-free bovine serum albumin (BSA) was obtained fromICN Biochemicals, (Cleveland, OH). The RNeasy Tissue kit was from Qiagen (Valencia, CA). The SuperScript® III First-Strand Synthesis System was purchased from Invitrogen (Carlsbad, CA). Real-time PCR reagents were acquired from Applied Biosystems (Foster City, CA). An antibody against CD36 was purchased from Thermo Scientific (Rockford, IL). Pierce ECL Western Blotting Substrate was purchased from Thermo Scientific (Rockford, IL). Insulin assay kit was obtained from Crystal Chem (Downers Grove, IL). Oil Red O solution was obtained from Electron Microscopy Science (Hatfield PA). Infinity™ Triglycerides kit was purchased from Fisher Diagnostics (Middletown, VA), total cholesterol assay kit was from Genzyme Diagnostics (Charlottetown, PE Canada) and NEFA-HR assay kits for free fatty acid was from Wako Bioproducts (Richmond, VA). A glucometer and test strips were purchased from LifeScan (Milpitas, CA). High-fat diet (60% kJ/fat, 20% kJ/carbohydrate, 20% kJ/protein) with/without additional 0.2% cholesterol was purchased from Bio-serv (Frenchtown, NJ). C57BL/6 mice were purchased from Charles River (Wilmington, MA).

Animals and treatment

All procedures performed on mice were approved by the Institutional Animal Care and Use Committee at the University of Georgia, Athens, Georgia. Fifteen-week-old male C57BL/6 mice were fed a high-fat diet with or without additional 0.2% cholesterol and received twice weekly injections of GW4064 (50 mg/kg, intra-peritoneal) or carrier solution [dimethyl sulfoxide (DMSO)] solution for 6 weeks. Animals were weighed weekly and their body composition was determined using EchoMRI-100™ from Echo Medical Systems (Houston, TX).

Cell culture

Mouse liver cells (BNL CL.2) were purchased from American Type Culture Collection (Manassas, VA) and maintained in a humidified incubator under 5% CO_2 at 37°C in

Dulbecco's Modified Eagle's Medium (DMEM) supplemented with 10% fetal bovine serum (FBS) and 1% penicillin/streptomycin. When cells were divided into six-well plates and reached ~90% confluence, sub-confluent cells were washed three times with phosphate buffered saline (PBS) and replaced with serum-free DMEM supplemented with 1% fatty acid-free BSA. Oleic acid (final concentration 500 μM) and GW4064 at various concentrations were added and incubated for 24 h. Cells were then fixed with 4% formaldehyde for Oil Red O staining or harvested for protein and western blot analysis.

Histochemical analysis

After mice were sacrificed, the liver and white and brown adipose tissues were collected, fixed in 10% formalin, embedded in paraffin, and sectioned at a thickness of 5 μm. Hematoxylin and eosin (H&E) staining were performed. Frozen sections (9 m) were stained with 0.2% Oil Red O in 60% of 2-propanol for 10 min and washed three times with PBS. Microscopic examination was performed, and photographs were taken under a regular light microscope.

Lipid extraction and analysis

Liver tissues were homogenized in PBS and protein concentration was determined. Total lipids in 300 μl of homogenate were extracted by addition of 5 ml of chloroform-methanol (2:1, vol/vol) mixture. An aliquot of the organic phase was evaporated to dry and resolved in 2% Triton X-100. Hepatic cholesterol, triglyceride, and free fatty acid assays were performed according to the manufacturer's instructions.

Analysis of serum lipids and insulin levels

Blood samples were collected from fasted mice. Cholesterol, triglyceride, free fatty acid and insulin levels in the plasma were measured using commercial assay kits according to the manufacturer's instructions.

Glucose tolerance test (GTT)

For GTT, mice were injected intraperitoneally with glucose at 2g/kg body weight after fasting overnight. Blood samples were taken at varying time points and glucose concentrations were measured using a glucometer.

Gene expression analysis by real time PCR

Total RNA was isolated from the mouse liver and white and brown adipose tissues using an RNeasy kit. Two μg of total RNA were used for the first strand cDNA synthesis, as recommended by the manufacturer (Invitrogen, Carlsbad, CA). Real time PCR (RT-PCR) was performed using SYBR Green as an indicator on the ABI StepOne Plus Real-Time PCR system. The final reaction mixture contained 20 ng of cDNA, 250 nM of each primer, 10 μl of 2x SYBR Green PCR Master, and RNase-free water to complete the reaction mixture volume to 20 μl. PCR was carried out for 40 cycles at 95°C for 15 sec and 60°C for 1 min. Fluorescence was read during the reaction, allowing a continuous monitoring of the amount of PCR product. The data were normalized to internal control GAPDH mRNA. The primer sequences employed are summarized in Table 1.

Western blot analysis

Fifty micrograms of total proteins were separated on 10% SDS-PAGE gels and transferred onto a polyvinylidene difluoride membrane using a Bio-Rad Mini-Blot transfer apparatus. Membranes were blocked in Tris-buffered solution (TBS) containing 5% nonfat dried milk for 1 h. The immunoblotting was performed at 4°C overnight with shaking using antibodies against CD36 at 1:1000 dilution. After being washed, the membrane was incubated in a

1:3,000 dilution of a secondary antibody (goat anti-rabbit IgG-HRP conjugate) at room temperature for 1 h in Tris-buffered saline containing 0.5% of Tween-20. Protein bands were visualized using Pierce ECL Western Blotting Substrate.

Statistical analysis

Statistical analysis was performed by one-way ANOVA. All data are reported as mean ± standard deviation (SD) with statistical significance set at $P<0.05$.

Results

FXR agonist GW4064 suppresses diet-induced obesity in mice

To investigate the role of FXR activation in diet-induced obesity, fifteen-week-old male C57BL/6 mice were fed a high-fat diet (HFD) with or without 0.2% cholesterol while being treated with either DMSO (vehicle) or GW4064 (50 mg/kg, twice weekly) for 6 weeks. As expected, HFD feeding induced a progressive increase in body weight (**Figure 1A**). GW4064 significantly attenuated the increase in weight gain. A statistical difference was evidenced as early as the first three weeks of HFD-feeding and the difference in body weight was 6.5 g between treated and control animals at the end of experiment. Considering the function of FXR in cholesterol metabolism, we also assessed whether FXR activation has different effects on mice fed with extra dietary cholesterol (HFD-Chol). As shown in **Figure 1B**, GW4064 also suppressed the gain of body weight when 0.2% cholesterol was included in the HFD. There was also 5.2 g difference in body weight between GW4064-treated and control animals at the end of 6-week treatment. Difference in body weight between DMSO- and GW4064-treated groups was due to a slight, but significantly reduction in fat and lean mass (**Figures 1C, 1D**), while the food intake was unchanged among the groups as shown in **Figures 1E** and **1F**. In addition, hematoxylin and eosin (H&E) staining showed no obvious difference in adipocyte size in both WAT and BAT (**Figure 1G, 1H**) between control and GW4064-treated animals. These results suggest that GW4064 does not block but significantly suppressed the gain of body weight in animals on HFD with or without inclusion of extra cholesterol.

GW4064 represses hepatic steatosis and plasma lipid level in HFD-fed mice

Hepatic steatosis is frequently observed in obesity (17). To investigate whether activation of FXR by GW4064 prevents hepatic lipid accumulation, liver weight was measured after mice were sacrificed at the end of treatment. As shown in **Figures 2A** and **2B**, the average liver weight of control animals on HFD is 1.6 g compared to about 2.1 g for animals fed with HFD-Chol. Importantly, with GW4064 treatment, the average liver weight from both groups is about 1.2 g, and 1.3 g, 0.4 and 0.8 g less than that of controls with or without extra cholesterol included, respectively. H&E staining of liver sections shows extensive vacuolation in control animals (**Figures 2C and 2E**) but not in those treated (**Figures 2D and 2F**) with GW4064. Oil Red O-staining confirms massive presence of fatty components in liver sections in animals on HFD (**Figure 2G**) and HFD-Chol (**Figure 2I**). In contrast, Oil Red O staining of liver sections displayed significantly less fat accumulation in GW4064 treated groups (**Figures 2H, 2J**).

Consistent with the results from the liver sections, treatment of mice with GW4064 significantly reduced hepatic triglyceride (**Figure 3A**) and free fatty acid (**Figure 3B)** levels in animals fed with HFD and HFD-Chol. As expected, the overall cholesterol level in the liver of animals fed with HFD-Chol is higher than that of animals on regular HFD (**Figure 3C**). GW4064 treatment also slightly brought down the cholesterol level in both cases.

The effects of GW4064 on serum concentration of triglyceride, free fatty acids and cholesterol were also examined. Results in **Figures 3D** and **3F** show significantly lower concentrations of triglyceride and cholesterol in GW4064 treated animals. There is no statistical difference in serum concentration of free fatty acids in animals with or without GW4064 treatment (**Figure 3E**). Taken together, these data demonstrate that activation of FXR by GW4064 markedly reduces hepatic lipid levels and improves the plasma lipid profile of mice on HFD.

GW4064 attenuated diet-induced hepatic inflammation

It is well known that obesity is a chronic inflammatory disease. Dietary cholesterol is an important risk factor for liver inflammation (18, 19). Therefore, we examined whether the protective effect of GW4064 on the liver involves suppression of hepatic inflammation. Results in **Figure 4A** showed elevated expression by 1.8-2.2 folds of macrophage marker genes including *F4/80, Cd68, Cd11c*, and *Cd11b* in mice fed HFD-Chol compared to those fed regular HFD. Compared to the HFD-fed group, cholesterol also enhanced gene expression of chemokine monocyte chemo-attractant protein-1 (*Mcp-1*) by 3.7-fold and pro-inflammatory factor *Il-1*β and *TNF*α by 1.8- and 4.4-fold, respectively (**Figure 4B**). GW4064 treatment significantly suppressed the diet-induced increase of inflammatory mediators, as evidenced by reduced macrophage markers and decreased inflammatory factor levels in liver. It is noted that GW4064 treatment did not affect mRNA levels of the same class of genes in white adipose tissue (WAT) (**Figures 4C, D**), indicating GW4064-activated FXR did not block macrophage infiltration into WAT. These data suggest that GW4064 treatment significantly reduces hepatic inflammation associated with HFD and HFD-Chol feeding.

GW4064 prevented lipid accumulation in liver through reducing CD36 expression

To determine how GW4064 treatment reduces excess lipid accumulation in the liver, the expression profiles of genes that are involved in lipid metabolism were analyzed. As shown in **Figure 5A**, GW4064 failed to inhibit lipogenesis in diet-induced obese mice, as evidenced by unchanged expression of sterol regulatory element-binding protein 1c (*Srebp-1c*), acetyl-CoA carboxylase1 (*Acc1*) and even up-regulated stearoyl CoA desaturase 1(S*cd-1*). The mRNA level of peroxisome proliferator-activated receptor alpha (*Ppar*-α) also did not significantly change. However, GW4064 markedly reduced the mRNA level of *Cd36* by 37% in HFD-fed and by 60% in HFD-Chol-fed animals. Western blot analysis of liver extract (**Figure 5B**) showed that CD36 protein level was also decreased in GW4064-treated animals.

To ascertain that a decrease of CD36 expression contributes to the reduction of hepatic lipid accumulation by GW4064 treatment, a similar *in vitro* study was performed in a mouse liver cell line (BNL Cl.2). As shown in **Figure 6A**, incubation of cells with oleic acid (500 μM) clearly increased the number of lipid droplets compared to the DMSO-treated control group. Treatment with different concentrations of GW4064 reduced the lipid accumulation in the cells. Concordantly, GW4064 treatment significantly repressed oleic acid-induced CD36 protein levels in a dose-dependent manner (**Figure 6B**). Taken together, these data indicate that prevention of hepatic lipid accumulation is likely due to an inhibition of *Cd36* expression by long-term GW4064 treatment.

Improvement of diet-induced hyperinsulinemia and hyperglycemia by GW4064 treatment

Obesity is a strong risk factor for insulin resistance, a characteristic of type-2 diabetes. We then investigated whether FXR activation by GW4064 would affect glucose homeostasis. Compared to HFD-fed animals, inclusion of extra dietary cholesterol in HFD induced higher plasma glucose levels (235±15 vs. 195±21; p=0.02). However, glucose tolerance tests

(**Figures 7A**, 7**C**) and calculated area under the curve (AUC) (**Figures 7B,** 7**D**) showed a much quicker clearance rate of intra-peritoneally injected glucose in GW4064-treated animals, indicating activation of FXR by GW4064 could maintain plasma glucose level. GW4064 also ameliorated diet-induced hyperinsulinemia (**Figure 7E**) and similar patterns were obtained by HOMA-IR (**Figure 7F**). These results demonstrate that GW4064 treatment prevents the progression of insulin resistance in animals on HFD with or without extra cholesterol.

To investigate how GW4064 treatment maintains glucose levels in animals, we measured the expression of genes involved in hepatic gluconeogenesis after mice were sacrificed. Results in **Figure 7G** from real-time PCR revealed that GW4064 treatment significantly lowered the amount of transcript for phosphoenolpyruvate carboxykinase (*Pepck*) and glucose-6-phosphatase (*G6pase*), concordant with reduction of diet-induced hyperglycemia and hyperinsulinemia.

Discussion

The current study demonstrates that activation of FXR by GW4064 reduced weight gain in mice fed a HFD with or without excess cholesterol (**Figures 1A and 1B**) included. GW4064 treatment significantly curbed HFD-induced hepatic steatosis as evidenced by lower level of triglyceride, free fatty acid and cholesterol in the liver (**Figures 2 and 3A-3C**). RT-PCR analysis revealed that GW4064 treatment attenuated hepatic inflammation but had no effect on white adipose tissue (**Figure 4**). GW4064 treatment markedly reduced expression of lipid transporter CD36 (**Figure 5, Figure 6**) without affecting expression of genes directly involved in lipogenesis. In addition, activation of FXR by GW4064 blocked diet-induced hyperinsulinemia and hyperglycemia through decreasing transcription of phosphoenolpyruvate carboxykinase (*Pepck*) and glucose-6-phosphatase (*G6pase*), two key enzymes in gluconeogenesis (**Figure 7**). These results provide direct evidence in support that FXR activation can be considered as an effective mean in blocking high fat diet-induced hepatic steatosis and insulin resistance.

HFD-Chol was included in the study because FXR is known for its function in cholesterol metabolism, hepatic steatosis and inflammation (18-21). With 6-week feeding, extra amounts of cholesterol in HFD did not further increase animal body weight compared to those fed with HFD, suggesting that dietary cholesterol does not play critical role in animal growth when on HFD. However, addition of cholesterol markedly enhanced hepatic steatosis as evidenced by an increase in liver weight and lipid content. HFD-Chol also enhanced hepatic inflammation as evidenced by elevated mRNA level of macrophage markers and pro-inflammatory factors (**Figure 4**). Mice fed a HFD-Chol also had much higher plasma glucose concentrations compared to that of animals fed a HFD. These results suggest that dietary cholesterol has a significant influence on lipid metabolism in the liver.

Results in **Figures 2** and **3** clearly show that GW4064 prevented liver steatosis by reducing hepatic lipid accumulation. In addition, activation of FXR also markedly attenuated mRNA levels of macrophage markers and pro-inflammatory mediators in the liver, in agreement with a previous study using WAY-362450 as a FXR activator in mice fed a methionine and choline-deficient diet (22). As for the mechanism through which FXR exerts its hypotriglyceridemic effect, the major function of FXR is to inhibit lipogenesis (9). For example, the study in Zucker (*fa/fa*) rats fed with standard diet showed FXR agonist 6-ethyl-chenodeoxycholic acid (6E-CDCA) protected agonist hepatic steatosis by inhibiting expression of S*rebp-1* and its target gene fatty acid synthase (*Fas*), the key genes involved in lipogenesis (12).

CD36 is responsible for the transport of long-chain fatty acids into the adipose and hepatic tissues (23, 24). Increased hepatic CD36 activity is critical for the development of steatosis in obesity (25-27). Results in **Figure 5** show that expression of *Cd36* is significantly reduced in GM4064-treated animals at both mRNA and protein level, suggesting that high level of CD36 plays an important role in HFD-induced hepatic steatosis. To provide additional evidence in support of such a possibility, we cultured BNLC1.2 cells in presence of varying amounts of GW4064, and the results in **Figure 6** clearly show that GW4064 concentration used in treatment is reversely proportional to the lipid levels in cultured cells (**Figure 6A**) and CD36 protein levels (**Figure 6B**) in the presence of 500 μM oleic acids. It is likely that GW4064-mediated inhibition of hepatic steatosis is achieved by reducing CD36 activity at mRNA and protein levels. Concordant with our results, other groups also reported that GW4064 significantly reverted HIV p17 protein-induced *Cd36* mRNA level in THP-1 macrophages (28) and treatment with other FXR agonist INT-747 resulted in a robust reduction of CD36 expression on circulating macrophages in ApoE$^{-/-}$ mice (29). In addition, recent studies revealed that HFD significantly induced CD36 expression in the liver (27, 30) and enhanced adipose tissue and liver inflammation. CD36 knockout mice showed a repression in hepatic inflammation (31, 32). Therefore, reduction of diet-induced CD36 expression by GW4064 may also help to ameliorate hepatic inflammation.

It is known that FXR activation affects lipid metabolism at different levels. For example, GW4064 inhibits lipogenesis by suppressing expression of *Srebp1c* and its target genes in mice fed a regular chow (9,11). It has also been shown that FXR$^{-/-}$ mice have normal or reduced hepatic *Srebp1c* expression (33 34). Activation of FXR was found to be able to enhance PPARα activity and increase triglyceride clearance (35). In addition, the effect of GW4064 treatment is time dependent. Cholic acid-induced FXR activation ameliorates expression of genes involving in lipogenesis in C57BL/6 mice one day after the GW4064 treatment, but the inhibitory effect was not seen after treatment for 7 days (9). The results summarized in this study suggest that activation of FXR by GW4064 in mice fed a high-fat diet blocks liver steatosis by suppressing expression of CD36 gene encoding fatty acid transporter.

GW4064 treatment prevented HFD-induced hyperglycermia and hyperinsulinma (**Fiugre 7**). Such activity is co-related to a lower mRNA level of *Pepck* and *G6pase*, two key genes in gluconeogenesis, in agreement with previous report in *db/db* mice (11). It remains to be elucidated how FXR activation improves insulin sensitivity. It is conceivable that FXR exerts an indirect effect on insulin sensitization by decreasing lipid levels as FXR is not expressed in skeletal muscle and at very low level in white adipose tissue. Since lipotoxicity could impair insulin signaling at the peripheral level (36), reduction of hepatic and plasma lipid levels may contribute to improving insulin sensitivity.

The detailed mechanism for GM4064 effect on animals fed a high fat diet remains to be elucidated. We believe that GW4064-activated FXR may suppress CD36 expression by inhibiting liver X receptor (LXR) activation. It is known that FXR and LXR, both serving as intracellular sensors, often oppose each other's action in order to maintain a balance for cholesterol and fat metabolism (37). It has been shown, using chenodeoxycholic acid as FXR activator, that activated FXR induces small heterodimer partner (SHP) gene expression, decreases scavenger receptor class B, type I (SR-B1) gene expression, and inhibits LXR and liver receptor homolog-1 (*LRH-1*) activation (38). Since *Cd36* is a target gene of LXR (39), it is highly possible that GW4064-activated FXR suppresses *Cd36* expression by inhibiting LXR activation.

In addition, *Scd-1* is generally considered as pro-lipogenic gene encoding SCD1 serving as a rate-limiting enzyme for converting saturated fatty acids to monounsaturated fatty acids.

Recent study showed that enhanced SCD1 activity in liver is associated with low fat content in healthy subjects under a lipogenic diet (40). Increase in *Scd-1* mRNA level (Figure 5A) suggests that chronic activation of FXR by GW4064 in mice fed a high fat diet could reduce the level of saturated fatty acids, and thereby, preventing deleterious lipotoxicity induced by the saturated fatty acids.

In summary, we demonstrate in the current study that GW4064-mediated FXR activation ameliorates diet-induced obesity, suppresses hepatic lipid accumulation, and maintains glucose and lipid homeostasis in C57BL/6 mice. These results suggest that the pharmacological activation of FXR represents a promising therapeutic strategy for treatment of obesity-associated liver steatosis.

Acknowledgments

The authors would like to thank Ms. Ryan Fugett for critical and proof read the manuscript.

Grants

This work was supported in part by the National Institute of Health [RO1EB007357 and RO1HL098295].

References

1. Zhang Y, Kast-Woelbern HR, Edwards PA. Natural structural variants of the nuclear receptor farnesoid X receptor affect transcriptional activation. J Biol Chem. 2003; 278:104–110. [PubMed: 12393883]
2. Wang H, Chen J, Hollister K, Sowers LC, Forman BM. Endogenous bile acids are ligands for the nuclear receptor FXR/BAR. Mol Cell. 1999; 3:543–553. [PubMed: 10360171]
3. Makishima M, Okamoto AY, Repa JJ, Tu H, Learned RM, Luk A, Hull MV, Lustig Mangelsdorf DJ, Shan B. Identification of a nuclear receptor for bile acids. Science. 1999; 284:1362–1365. [PubMed: 10334992]
4. Kok T, Hulzebos CV, Wolters H, Havinga R, Agellon LB, Stellaard F, Shan B, Schwarz Kuipers F. Enterohepatic circulation of bile salts in farnesoid x receptor-deficient mice -Efficient intestinal bile salt absorption in the absence of ileal bile acid-binding protein. J Biol Chem. 2003; 278:41930–41937. [PubMed: 12917447]
5. Sinal CJ, Tohkin M, Miyata M, Ward JM, Lambert G, Gonzalez FJ. Targeted disruption of the nuclear receptor FXR/BAR impairs bile acid and lipid homeostasis. Cell. 2000; 102:731–744. [PubMed: 11030617]
6. Holt JA, Luo GZ, Billin AN, Bisi J, McNeill YY, Kozarsky KF, Donahee M, Wang DY, Mansfield TA, Kliewer SA, Goodwin B, Jones SA. Definition of a novel growth factordependent signal cascade for the suppression of bile acid biosynthesis. Gene Dev. 2003; 17:1581–1591. [PubMed: 12815072]
7. Claudel T, Inoue Y, Barbier O, Duran-Sandoval D, Kosykh V, Fruchart J, Fruchart JC, Gonzalez FJ, Staels B. Farnesoid X receptor agonists suppress hepatic apolipoprotein CIII expression. Gastroenterology. 2003; 125:544–555. [PubMed: 12891557]
8. Kast HR, Nguyen CM, Sinal CJ, Jones SA, Laffitte BA, Reue K, Gonzalez FJ, Willson TM, Edwards PA. Farnesoid X-activated receptor induces apolipoprotein C-II transcription: a molecular mechanism linking plasma triglyceride levels to bile acids. Mol Endocrinol. 2001; 15:1720–1728. [PubMed: 11579204]
9. Watanabe M, Houten SM, Wang L, Moschetta A, Mangelsdorf DJ, Heyman RA, Moore DD, Auwerx J. Bile acids lower triglyceride levels via a pathway involving FXR, SHP, and SREBP-1c. J Clin Invest. 2004; 113:1408–1418. [PubMed: 15146238]
10. Ma K, Saha PK, Chan L, Moore DD. Farnesoid X receptor is essential for normal glucose homeostasis. J Clin Invest. 2006; 116:1102–1109. [PubMed: 16557297]

11. Zhang Y, Lee FY, Barrera G, Lee H, Vales C, Gonzalez FJ, Willson TM, Edwards PA. Activation of the nuclear receptor FXR improves hyperglycemia and hyperlipidemia in diabetic mice. Proc Natl Acad Sci U S A. 2006; 103:1006–1011. [PubMed: 16410358]
12. Cipriani S, Mencarelli A, Palladino G, Fiorucci S. FXR activation reverses insulin resistance and lipid abnormalities and protects against liver steatosis in Zucker (fa/fa) obese rats. J Lipid Res. 2010; 51:771–784. [PubMed: 19783811]
13. Cariou B, van Harmelen K, Duran-Sandoval D, van Dijk TH, Grefhorst A, Abdelkarim M, Caron S, Torpier G, Fruchart JC, Gonzalez FJ, Kuipers F, Staels B. The farnesoid X receptor modulates adiposity and peripheral insulin sensitivity in mice. J Biol Chem. 2006; 281:11039–11049. [PubMed: 16446356]
14. Prawitt J, Abdelkarim M, Stroeve JHM, Popescu I, Duez H, Velagapudi VR, Dumont J, Bouchaert E, van Dijk TH, Lucas A, Dorchies E, Daoudi M, Lestavel S, Gonzalez FJ, Oresic M, Cariou B, Kuipers F, Caron S, Staels B. Farnesoid X receptor deficiency improves glucose homeostasis in mouse models of obesity. Diabetes. 2011; 60:1861–1871. [PubMed: 21593203]
15. Zhang YQ, Ge XM, Heemstra LA, Chen WD, Xu JS, Smith JL, Ma HY, Kasim N, Edwards PA, Novak CM. Loss of FXR protects against diet-induced obesity and accelerates liver carcinogenesis in ob/ob mice. Mol Endocrinol. 2012; 26:272–280. [PubMed: 22261820]
16. Maloney PR, Parks DJ, Haffner CD, Fivush AM, Chandra G, Plunket KD, Creech KL, Moore LB, Wilson JG, Lewis MC, Jones SA, Willson TM. Identification of a chemical tool for the orphan nuclear receptor FXR. J Med Chem. 2000; 43:2971–2974. [PubMed: 10956205]
17. Perlemuter G, Bigorgne A, Cassard-Doulcier AM, Naveau S. Nonalcoholic fatty liver disease: from pathogenesis to patient care. Nat Clin Pract Endocrinol Metab. 2007; 3:458–469. [PubMed: 17515890]
18. Subramanian S, Goodspeed L, Wang SR, Kim J, Zeng LX, Ioannou GN, Haigh WG, Yeh MM, Kowdley KV, O'Brien KD, Pennathur S, Chait A. Dietary cholesterol exacerbates hepatic steatosis and inflammation in obese LDL receptor-deficient mice. J Lipid Res. 2011; 52:1626–1635. [PubMed: 21690266]
19. Savard C, Tartaglione EV, Kuver R, Geoffrey WH, Farrell GC, Subramanian S, Chait A, Yeh MM, Quinn LS, Ioannou GN. Synergistic interaction of dietary cholesterol and dietary fat in inducing experimental steatohepatitis. Hepatology. 2012 doi:10.1002/hep.25789.
20. Savard C, Tartaglione EV, Kuver R, Geoffrey WH, Farrell GC, Subramanian S, Chait A, Yeh MM, Quinn LS, Ioannou GN. Synergistic interaction of dietary cholesterol and dietary fat in inducing experimental steatohepatitis. Hepatology. 2012 doi:10.1002/hep.25789.
21. Wouters K, van Gorp PJ, Bieghs V, Gijbels MJ, Duimel H, Lutjohann D, Kerksiek A, van Kruchten R, Maeda N, Staels B, van Bilsen M, Shiri-Sverdlov R, Hofker MH. Dietary cholesterol, rather than liver steatosis, leads to hepatic inflammation in hyperlipidemic mouse models of nonalcoholic steatohepatitis. Hepatology. 2008; 48:474–486. [PubMed: 18666236]
22. Zhang S, Wang J, Liu Q, Harnish DC. Farnesoid X receptor agonist WAY-362450 attenuates liver inflammation and fibrosis in murine model of non-alcoholic steatohepatitis. J Hepatol. 2009; 51:380–388. [PubMed: 19501927]
23. Hajri T, Hall AM, Jensen DR, Pietka TA, Drover VA, Tao H, Eckel R, Abumrad NA. CD36-facilitated fatty acid uptake inhibits leptin production and signaling in adipose tissue. Diabetes.
24. Coburn CT, Knapp FF, Febbraio M Jr. Beets AL, Silverstein RL, Abumrad NA. Defective uptake and utilization of long chain fatty acids in muscle and adipose tissues of CD36 knockout mice. J Biol Chem. 2000; 275:32523–32529. [PubMed: 10913136]
25. Kim Y, Park T. DNA microarrays to define and search for genes associated with obesity. Biotechnol J. 2010; 5:99–112. [PubMed: 20024972]
26. Miquilena-Colina ME, Lima-Cabello E, Sanchez-Campos S, Garcia-Mediavilla MV, Fernandez-Bermejo M, Lozano-Rodriguez T, Vargas-Castrillon J, Buque X, Ochoa B, Aspichueta P, Gonzalez-Gallego J, Garcia-Monzon C. Hepatic fatty acid translocase CD36 upregulation is associated with insulin resistance, hyperinsulinaemia and increased steatosis in non-alcoholic steatohepatitis and chronic hepatitis C. Gut. 2011; 60:1394–1402. [PubMed: 21270117]

27. Koonen DPY, Jacobs RL, Febbraio M, Young ME, Soltys CLM, Ong H, Vance DE, Dyck JRB. Increased hepatic CD36 expression contributes to dyslipidemia associated with dietinduced obesity. Diabetes. 2007; 56:2863–2871. [PubMed: 17728375]
28. Renga B, Francisci D, D'Amore C, Schiaroli E, Mencarelli A, Cipriani S, Baldelli F, Fiorucci S. The HIV matrix protein p17 subverts nuclear receptors expression and induces a STAT1-dependent proinflammatory phenotype in monocytes. PloS One. 2012; 7:e35924. 7. [PubMed: 22558273]
29. Mencarelli A, Renga B, Distrutti E, Fiorucci S. Antiatherosclerotic effect of farnesoid X receptor. Am J Physiol Heart Circ Physiol. 2009; 296:H272–H281. [PubMed: 19028791]
30. Ma Y, Liu D. Activation of pregnane X receptor by pregnenolone 16 alpha-carbonitrile prevents high-fat diet-induced obesity in AKR/J mice. PloS One. 2012; 7:e38734. [PubMed: 22723881]
31. Bieghs V, Verheyen F, van Gorp PJ, Hendrikx T, Wouters K, Lutjohann D, Gijbels MJ, Febbraio M, Binder CJ, Hofker MH, Shiri-Sverdlov R. Internalization of modified lipids by CD36 and SR-A leads to hepatic inflammation and lysosomal cholesterol storage in Kupffer cells. PloS One. 2012; 7:e34378. [PubMed: 22470565]
32. Cai L, Wang Z, Ji A, Meyer JM, van der Westhuyzen DR. Scavenger receptor CD36 expression contributes to adipose tissue inflammation and cell death in diet-induced obesity. PloS One. 2012; 7:e36785. [PubMed: 22615812]
33. Zhang Y, Castellani LW, Sinal CJ, Gonzalez FJ, Edwards PA. Peroxisome proliferator-activated receptor-gamma coactivator 1alpha (PGC-1alpha) regulates triglyceride metabolism by activation of the nuclear receptor FXR. Genes Dev. 2004; 18:157–169. [PubMed: 14729567]
34. Duran-Sandoval D, Cariou B, Percevault F, Hennuyer N, Grefhorst A, van Dijk TH, Gonzalez FJ, Fruchart JC, Kuipers F, Staels B. The farnesoid X receptor modulates hepatic carbohydrate metabolism during the fasting-refeeding transition. J Biol Chem. 2005; 280:29971–29979. [PubMed: 15899888]
35. Cariou B, Staels B. FXR: a promising target for the metabolic syndrome? Trends in pharmacological sciences. 2007; 28:236–243. [PubMed: 17412431]
36. Savage DB, Petersen KF, Shulman GI. Disordered lipid metabolism and the pathogenesis of insulin resistance. Physiol Rev. 2007; 87:507–520. [PubMed: 17429039]
37. Kalaany NY, Mangelsdorf DJ. LXRS and FXR: the yin and yang of cholesterol and fat metabolism. Annual review of physiology. 2006; 68:159–191.
38. Malerod L, Sporstol M, Juvet LK, Mousavi SA, Gjoen T, Berg T, Roos N, Eskild W. Bile acids reduce SR-BI expression in hepatocytes by a pathway involving FXR/RXR, SHP, and LRH-1. Biochem Biophys Res Commun. 2005; 336:1096–1105. [PubMed: 16168958]
39. Zhou J, Febbraio M, Wada T, Zhai Y, Kuruba R, He J, Lee JH, Khadem S, Ren S, Li S, Silverstein RL, Xie W. Hepatic fatty acid transporter *Cd36* is a common target of LXR, PXR, and PPARgamma in promoting steatosis. Gastroenterology. 2008; 134:556–567. [PubMed: 18242221]
40. Silbernagel G, Kovarova M, Cegan A, Machann J, Schick F, Lehmann R, Haring HU, Stefan N, Schleicher E, Fritsche A, Peter A. High Hepatic SCD1 Activity Is Associated with Low Liver Fat Content in Healthy Subjects under a Lipogenic Diet. J Clin Endocrinol Metab. 2012; 97:E2288–92. [PubMed: 23015656]

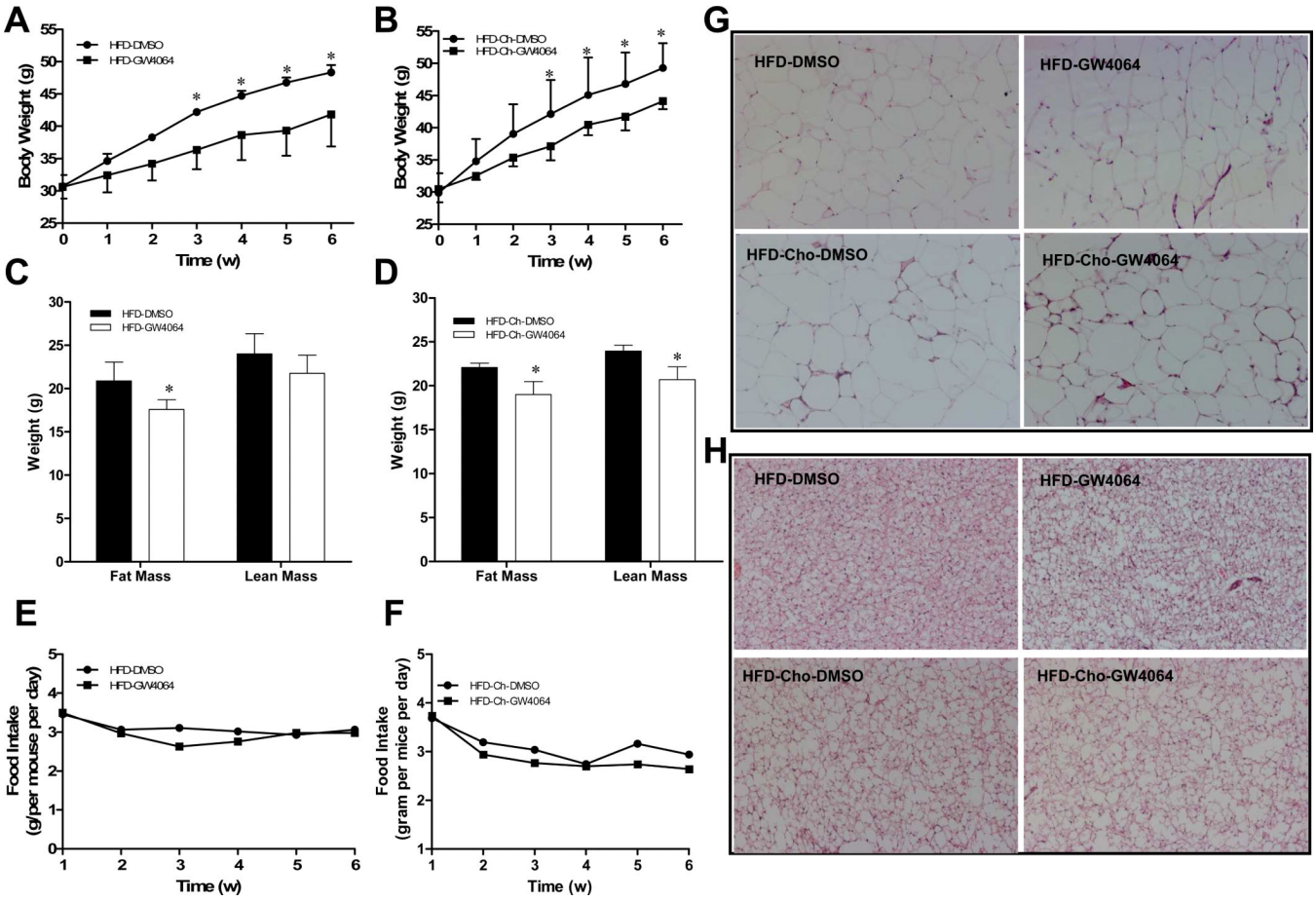

Figure 1. GW4064 treatment delays HFD-induced obesity in mice

Fifteen-week-old C57BL/6 mice (male) were fed with HFD with or without inclusion of 0.2% cholesterol for 6 weeks. Mice were intraperitoneally injected by GW4064 (50 mg/kg, twice weekly) or carrier solution (DMSO) as the control. **A, B**, growth curve; **C, D**, fat and lean mass; **E, F**, food intake; **G, H**, H&E staining of white and brown adipose tissue. Each data point represents the average ± SD of 4 animals. *P<0.05 compared to DMSO-treated control animals. HFD-DMSO, HFD-GW4064: mice were fed with high-fat diet and treated with DMSO or GW4064; HFD-Chol-DMSO, HFD-Chol-GW4064: mice were fed with high-fat diet with 0.2% cholesterol and treated with DMSO or GW4064.

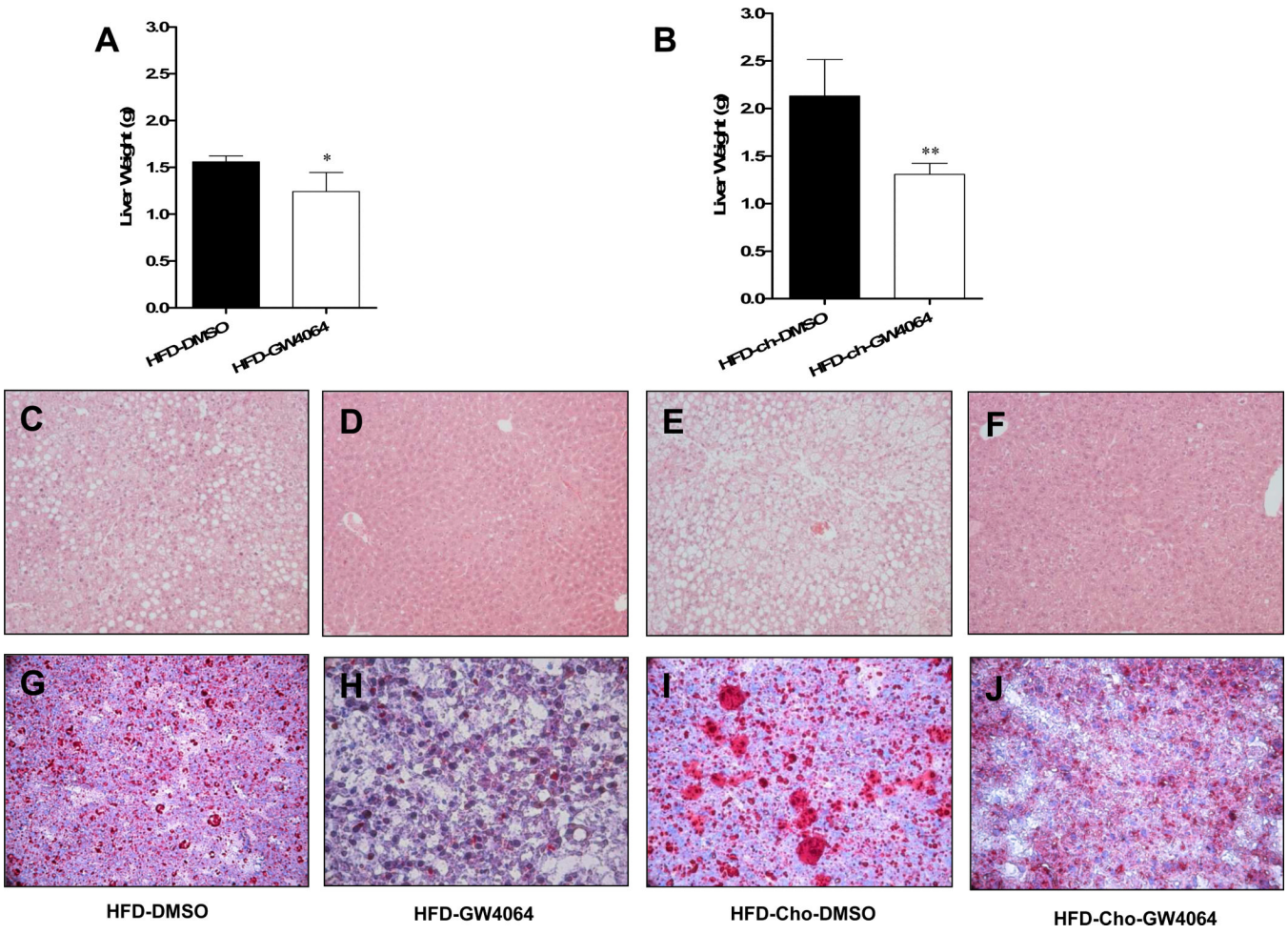

Figure 2. GW4064 repressed HFD-induced hepatic steatosis

At the end of the 6-week treatment, animals were sacrificed and liver weights were measured (**A, B**). Liver histology was evaluated by H&E staining (**C-F**, original magnifications 100×). Lipid accumulation was evaluated by Oil Red O staining (**G-J**, original magnifications 200×). HFD-DMSO, HFD-GW4064: mice were fed with high-fat diet and treated with DMSO or GW4064; HFD-Chol-DMSO, HFD-Chol-GW4064: mice were fed with HFD containing 0.2% cholesterol and treated with DMSO or GW4064. *P<0.05, **P<0.01 compared to DMSO-treated groups.

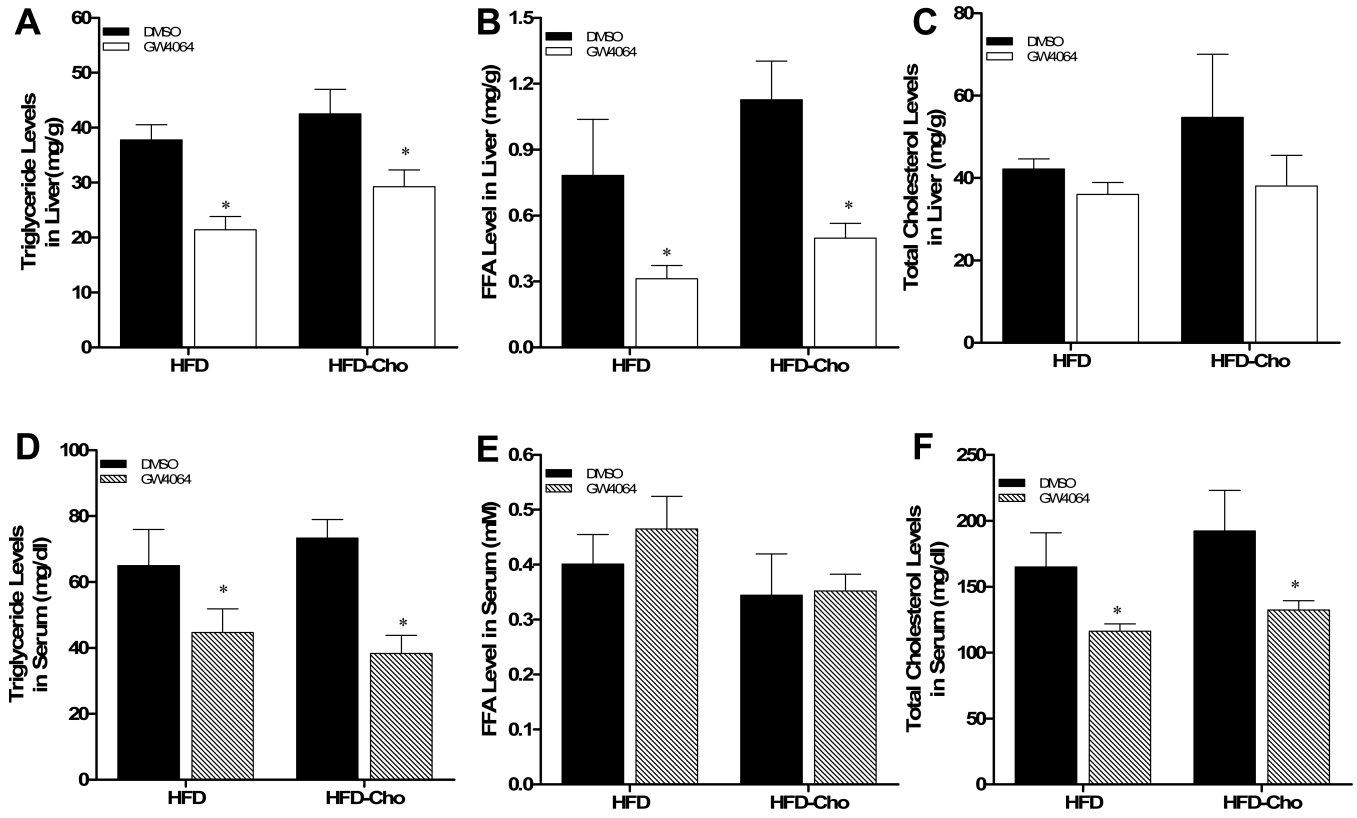

Figure 3. Reduction of hepatic and plasma lipid levels by GW4064 treatment in HFD-induced obese mice

(**A-C**) Triglyceride, free fatty acid and cholesterol content in the liver; (**D-F**) Serum levels of triglyceride, free fatty acid and cholesterol after 6-week treatment. Each data point represents the average ± SD of 4 animals in each group. *P<0.05, **P<0.01 compared to DMSO-treated groups

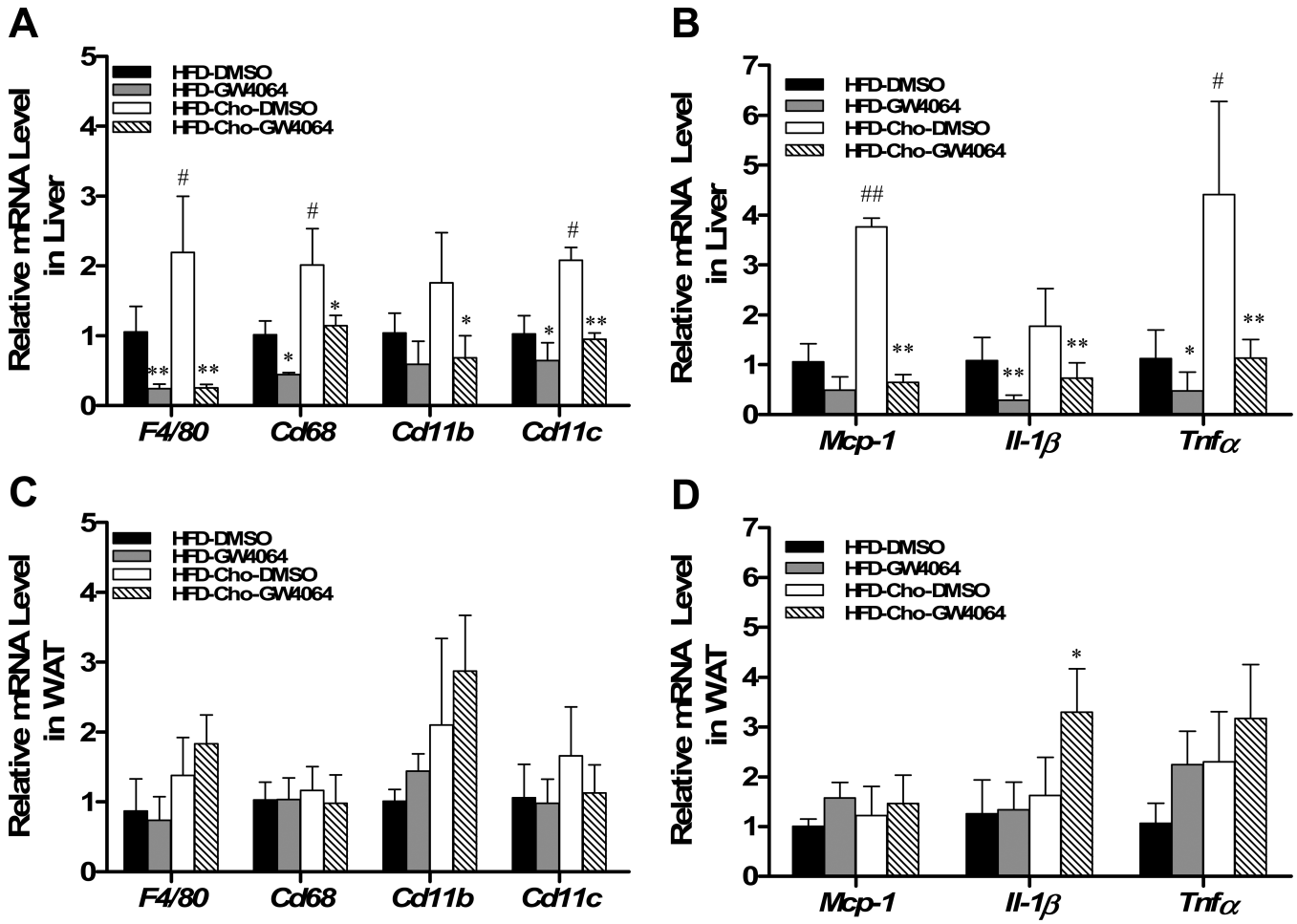

Figure 4. GW4064 attenuated HFD-induced hepatic inflammation

At the end of the sixth week, mice were treated with GW4064 or DMSO (carrier solution) and sacrificed 4 h later. Liver and WAT tissues were harvested and total RNA was extracted. Relative mRNA levels of selected genes were determined by real-time PCR. Macrophage markers *F4/80, Cd68, Cd11b*, and *Cd11c* in liver (**A**) and WAT (**C**); Cytokine gene expression for *Tnfα, Il-1β* and chemotactic factor genes *Mcp-1* in liver (**B**) and WAT (**D**); Each data point represents the average ± SD of 4 animals. *P<0.05, **P<0.01 compared to DMSO-treated groups; #P<0.05, ##P<0.01 compared to HFD-DMSO group

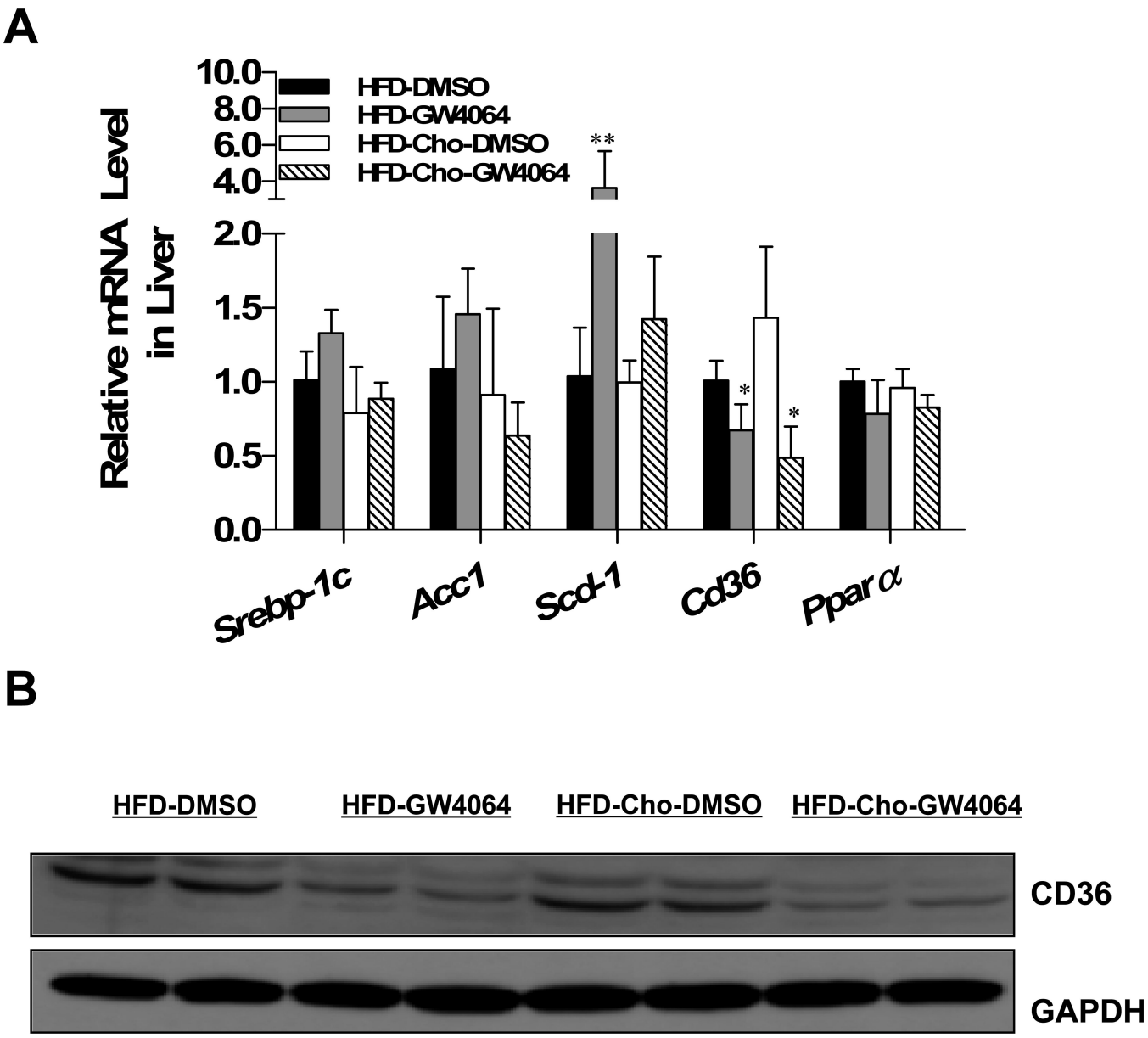

Figure 5. Effect of GW4064 treatment on expression of genes involved in lipogenesis and CD36 mRNA and protein expression

At the end of the 6-week treatment, mice were sacrificed and livers were harvested. The mRNA levels of *Srebp-1, Acc1, Scd-1, Cd36* and *Ppar*-α were examined by real-time PCR (**A**). CD36 protein level was determined by Western blot (**B**). Each data point represents the average ± SD of 4 animals. *P<0.05, **P<0.01 compared to DMSO-treated group.

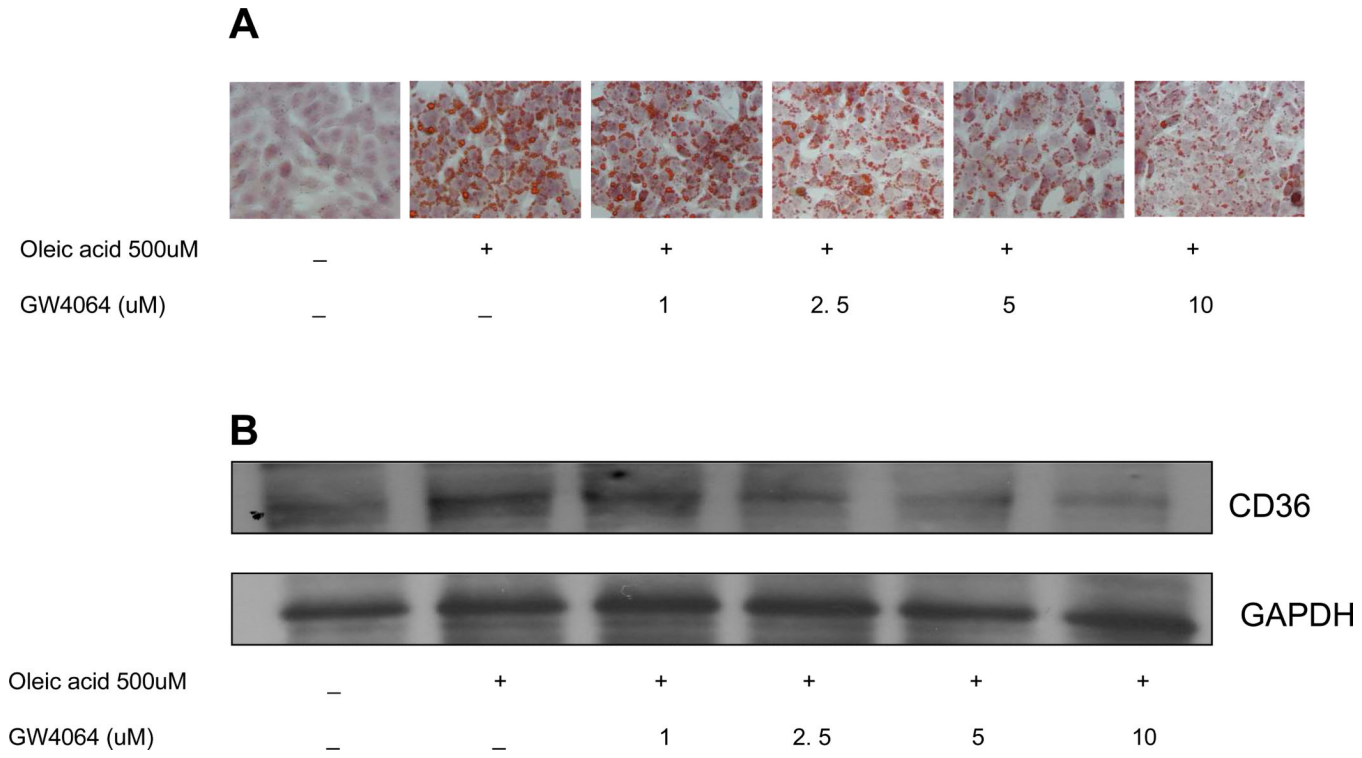

Figure 6. GW4064 reduced the oleic acid-induced lipids accumulation and CD36 protein level in liver cell line (BNL CL.2)

Mouse liver BNL-CL2 cells were incubated with 500 μM oleic acid and treated at different concentration of GW4064 for 24 h. Lipid accumulation in the cells was evaluated by Oil Red O staining (**A**). CD36 protein expression was detected by Western blot (**B**).

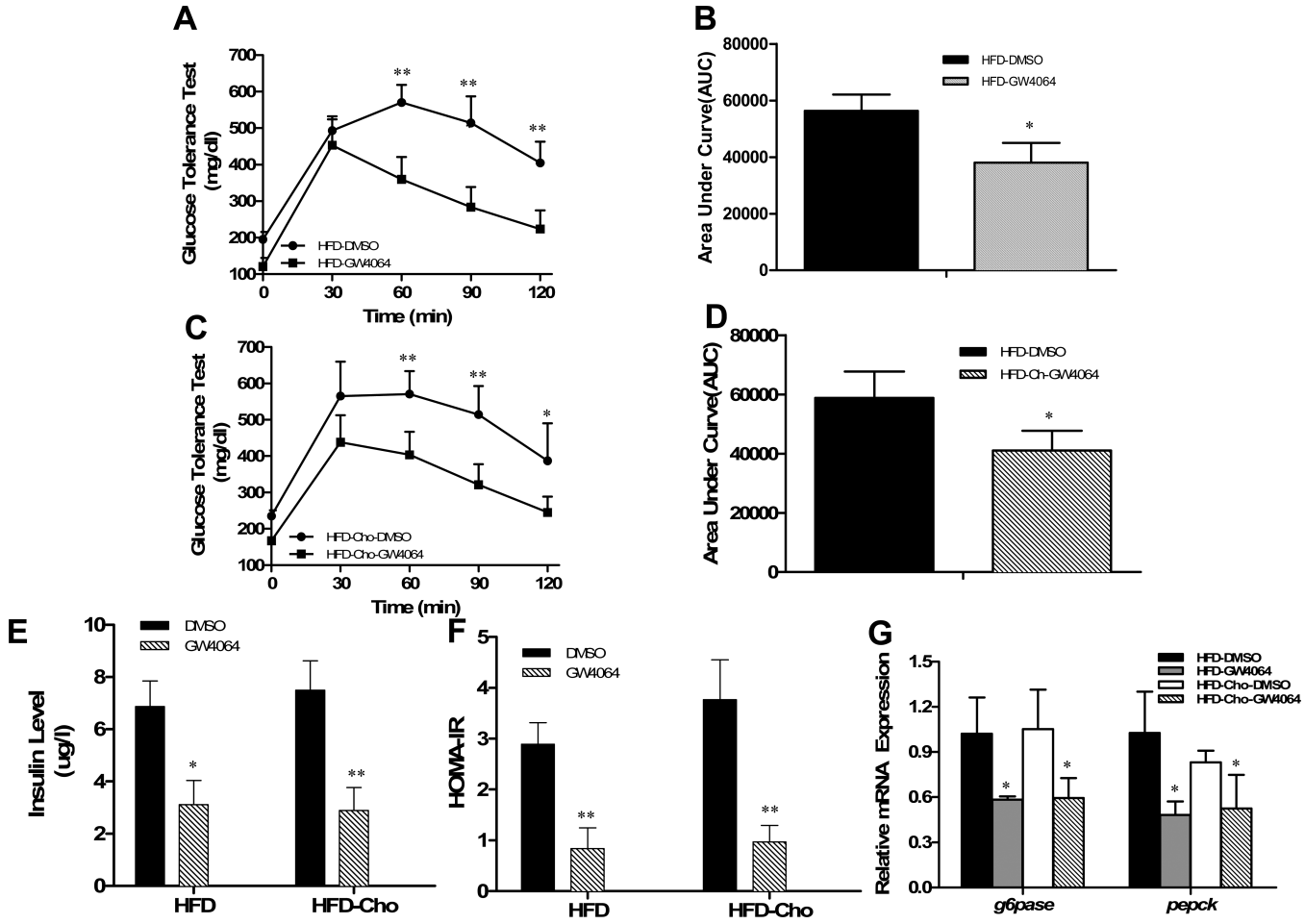

Figure 7. Effect of GW4064 treatment on glucose tolerance, serum concentration of insulin, and mRNA levels of G*6pase and Pepck*

Animals at the end of the 6-week treatment were fasted overnight for glucose tolerance tests. **A, C**, time-dependent blood concentration of glucose upon IP injection of glucose (2 g/kg); **B, D**, area under the curve from glucose tolerance test; **E**, insulin levels at the end of the 6-week feeding with or without GW4064 treatment; **F**, HOMA-IR values calculated based on formula: (fasting insulin [μU/ml] × fasting glucose [mmol/l]) / 22.5. **G**, relative mRNA levels of *G6pase* and *Pepck* in mouse liver at the end of animal feeding and GW4064 treatment. Each data point represents the average ± SD of 4 animals. *P<0.05, **P<0.01 compared to DMSO-treated groups.

Table 1

Primer sets for real time RT-PCR analysis of gene expression

Name	Forward sequence	Reverse sequence
Pepck	AAGCATTCAACGCCAGGTTC	GGGCGAGTCTGTCAGTTCAAT
G6pase	CGACTCGCTATCTCCAAGTGA	GTTGAACCAGTCTCCGACCA
Srebp-1c	CCCTGTGTGTACTGGCCTTT	TTGCGATGTCTCCAGAAGTG
Acc1	GCCTCTTCCTGACAAACGAG	TGACTGCCGAAACATCTCTG
Scd-1	TTCTTACACGACCACCACCA	CCGAAGAGGCAGGTGTAGAG
Cd36	CCTTAAAGGAATCCCCGTGT	TGCATTTGCCAATGTCTAGC
Ppar-α	TGTCGAATATGTGGGGACAA	AATCTTGCAGCTCCGATCAC
Cd68	CCATCCTTCACGATGACACCT	GGCAGGGTTATGAGTGACAGTT
F4/80	CCCCAGTGTCCTTACAGAGTG	GTGCCAGAGTGGATGTCT
Cd11b	ATGGACGCTGATGGCAATACC	TCCCCATTCACGTCTCCCA
Cd11c	ACGTCAGTACAAGGAGATGTTGGA	ATCCTATTGCAGAATGCTTCTTTACC
Mcp-1	ACTGAAGCCAGCTCTCTCTTCCTC	TTCCTTCTTGGGGTCAGCACAGAC
Il1-β	GAAATGCCACCTTTTGACAGTG	CTGGATGCTCTCATCAGGACA
Tnfα	CCCTCACACTCAGATCATCTTCT	GCTACGACGTGGGCTACAG
Gapdh	AGGTCGGTGTGAACGGATTTG	TGTAGACCATGTAGTTGAGGTCA